Available online at www.CivileJournal.org

Civil Engineering Journal

Vol. 4, No. 12, December, 2018

Study on Seismic Dynamic Response of Shallow-Buried Subway Station Structure and Ancillary Facilities

Miao Peng [a*], Jianwei Cui [b]

[a] *Department of Civil Engineering, Xiamen University of Technology, Xiamen, China.*

[b] *Department of Railway Engineering and Civil Engineering, Shandong Polytechnic, Jinan, China.*

Received 08 October 2018; Accepted 16 December 2018

Abstract

Strong earthquakes can cause damages to structural members and also yield non-negligible damages to nonstructural facilities, the latter being closely related to earthquake-induced inertial forces. At present, the acceleration response regularity of shallow-buried subway station structure is not very clear. Using the finite-element software ABAQUS, a dynamic soil-structure interaction model for a two-story subway station structure is established. The distribution of the peak acceleration response of the structure is obtained, and the damage assessment of non-structural facilities is carried out based on the structural acceleration response. The results demonstrate that, in general, the peak acceleration responses of the subway station structure increase from lower to upper story levels, while the peak acceleration responses at the same height are practically equal. Moreover, the peak accelerations of a shallow-buried subway station structure are generally less than or close to the peak ground acceleration. Furthermore, the nonstructural facilities are slightly damaged when subjected to a peak bedrock input acceleration of 0.1 g, and moderately damaged under a peak bedrock input acceleration in the range 0.2 – 0.6 g. Based on the acceleration response characteristics, it is proposed that the peak surface acceleration can be used as an index to evaluate the damage of non-structural facilities in shallow-buried subway station structure, which is simple, practical and basically meets the precision requirements.

Keywords: Subway Station Structure; Shallow-Buried Structure; Seismic Dynamic Response; Ancillary Facilities; Damage Evaluation.

1. Introduction

With the continuation of modern city development and underground space utilization, urban rail transit lines, which mainly consist of subways, have become an important means to resolve traffic problems. During the 1995 Great Hanshin earthquake in Japan, the Daikai, Luzawa, Nagata, and Sannomiya stations, suffered from various degrees of damage [1, 2]. In particular, the earthquake damage of Daikai subway station is extremely serious. It is the first large-scale underground structure earthquake damage case that has been completely destroyed in human history. A large number of theoretical, numerical and experimental research work has been carried out and the seismic damage mechanism and failure mode have been deeply and systematically analyzed [3]. The vibration table test can visually reveal the earthquake damage phenomenon. A multi-story subway station test was carried out to investigate the seismic effect. The result demonstrates that central columns are vulnerable components in multi-story subway stations [4]. The result of vibration table tests for subway station in loess soil shows that the Fourier spectrum values of accelerations increase at low-frequency components and decrease at high-frequency components form bottom to top of soil. The seismic responses of structure are controlled by surrounding soils in severe earthquake because of strong soil-structure interaction [5]. The seismic analysis results for the subway structures in soft soil area show that: The earthquake action

* Corresponding author: mpeng@xmut.edu.cn

http://dx.doi.org/10.28991/cej-03091203

in soft soil area is obvious，and the seismic effect in thick soft soil is much larger than that in thin soil. The mechanic property condition of the subway station can be considered as a flexible working stage [6]. Under multi-dimensional seismic wave action, a two-story subway station in Shanghai soft site was studied. The results show that the peak of structure internal force response, the ground acceleration response and displace response under long-period seismic waves are much bigger than the results under normal seismic waves [7]. Based on the typical soft soil condition in Tianjin, a three-dimensional finite element model for a two-story metro station structure was established. The seismic analysis results show that the deformation of the structure increases in the height direction. Alternately Dynamic tensile and compressive stresses occur at both the top and bottom of middle column with tensile plastic damage, indicating the middle column is the weakest component in the structure [8]. Three site soil classifications are designed, and the seismic deformation characteristics of the soil and metro structure interaction system are analyzed using the finite element method. The results show that the lateral soil always pushes the structure to produce the maximum relative deformation. The large deformation of the soil around the subway structure will adversely affect the seismic resistance of the structure [9]. The artificial treatment for semi-infinite boundary condition of subway structure's numeral model will directly influence the accuracy of analysis results. By using infinite-element method to simulate the numeral boundary, the characteristics of seismic wave passing through artificial boundary to semi-infinite region were simulated effectively. The infinite element boundary presents the advantage of simple technical processing, low computational cost and high precision. In the seismic analysis of subway station structures, it is feasible for coupling finite element with infinite element to simulate the soil area [10].

In addition to experiencing typical seismically induced structural damage, such as concrete spalling, steel rebar exposure, and plate wall cracking, subway stations also suffered from nonstructural member damage, such as mechanical and electrical pipeline damage, interior finish shedding, and facility overturning, causing enormous economic losses [11]. Therefore, as performance-based design philosophy is being applied to the seismic design of underground structures, damage to such nonstructural members should also be considered to avoid excessive economic losses.

It is difficult to directly estimate the damages to nonstructural members of a subway station. The damages to above-ground structures are generally described using appropriate structural response indices such as the inter-story drift angle to indirectly indicate the building damage and the floor acceleration response to indicate the damage to interior contents [12-14]. For the structure of a subway station, the structural deformation incurred during an earthquake causes damage to the decorative materials (e.g., ceramic tiles, fireproofing coatings, and decorative panels) on side walls, making the inter-story drift angle a good index with which to describe the damage to interior wall decoration. However, the lighting equipment, electrical facilities, and monitoring facilities within a subway station can be damaged by inertial forces during an earthquake, making the station acceleration response suitable to characterize the damage to such facilities. Because the inter-story drift angle can also be used as a structural damage index, the Code for Seismic Design of Buildings (GB50011-2010) in China has provided threshold values of inter-story drift angles for subway station structures designed at different seismic levels [15]. Although there has been relatively ample research on structural inter-story drift angles [16], research on the acceleration response of subway stations has been scarce.

The dynamic response of a subway station structure, as an underground concrete entity, is controlled not by the inertial forces of itself, but by the shear deformation of soil layers. Therefore, the acceleration response characteristics of a subway station structure are different from those of an above-ground structure. Using the general-purpose finite-element software ABAQUS (Dassault Systèmes, France), a two-story, two-span subway station is numerically modeled, and its dynamic time history considering soil-structure interaction is analyzed. The acceleration response characteristics of the subway station structure are summarized, based on which the damages to nonstructural members are evaluated.

2. Project Background

The two-story, two-span subway station considered in this study is an island-type station, which has an upper-story station floor and a lower-story island platform. Figure 1 shows the representative cross-sectional dimensions of the subway station structure, with a width of 21.84 m, a height of approximately 13.1 m, and a roof buried depth of 3.1 m. The station was constructed by the open-cut method, and its retaining structure was made of continuous underground walls. Inner lining walls were constructed in the station structure and were connected by embedded inserts to those continuous underground walls, thereby jointly resisting loads. The central columns in the two stories of the station have the same size, 1.4 m long and 0.7 m wide, with a column spacing of 8.5 m. The site category is Class III, and the soil layer has a shear wave velocity of 200 m/s, Poisson's ratio of 0.3, internal friction angle of 15°, and cohesion of 20 KPa. The soil density is 2000 kg/m^3, and the dynamic elastic modulus is $2.08 \times 10^3 \mathrm{N/m^2}$.

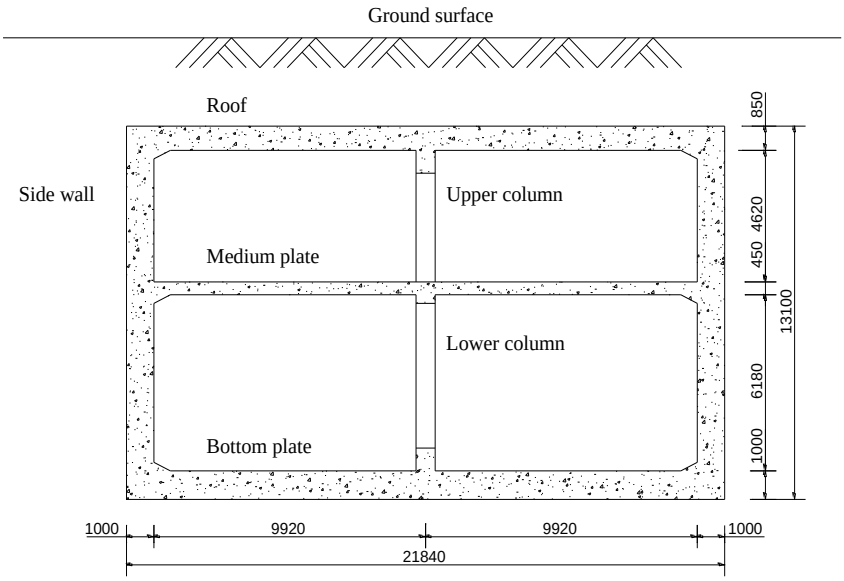

Figure 1. Representative cross-section (unit: mm)

3. Finite-Element Modeling

A numerical analysis model of soil-structure dynamic interaction was established by using finite element software ABAQUS. According to the plane strain problem analysis, the size of the structure is determined according to the axis of the standard cross section shown in Figure 1. According to the "Code for Seismic Design of Urban Rail Transit Structures" (GB50909-2014) and the "Code for Seismic Design of Buildings" (GB50011-2010), the distance between the side boundary of the model and the bottom boundary to the underground structure is not less than 3 times of the width and vertical effective height of the underground structure. In this paper, the width of one side of the soil is taken as 100 m, and the depth of the soil is taken to the top of the bedrock, which is 60 m. The dimensions meet the design specifications mentioned above.

The soil is simulated by the Mohr-Coulomb constitutive model with Rayleigh damping. The station structure is modeled using the beam element B21. The concrete material of the station structure adopts the material type C35. In order to better simulate the dynamic response of the structure as it enters the elastoplastic stage, the constitutive model of the structure takes the concrete plastic damage model (China Code GB50010-2010). This model uses the damage factors Dt and Dc to respectively describe the tensile and compressive damages degradation of concrete. The values of Dt and Dc are both in the range 0–1, with a larger value denoting more damage to an element and a value of 0 suggesting an elastic element. The steel reinforcement in reinforced concrete is simulated by an ideal elastoplastic model using the material type HRB400. It is reasonably assumed that the structure and the soil do not disengage or slip during their interaction under an earthquake.

The soil is simulated by the Mohr-Coulomb constitutive model while applying Rayleigh damping. Rayleigh damping is defined as follows:

$$C = \alpha M + \beta K \tag{1}$$

$$\alpha = 2\zeta\left(\frac{\omega_1\omega_2}{\omega_1 + \omega_2}\right) \tag{2}$$

$$\beta = 2\zeta\left(\frac{1}{\omega_1 + \omega_2}\right) \tag{3}$$

Among them, ω_1 and ω_2 are the first two orders of the natural vibration circle frequency, which is the damping ratio.

The lateral boundary of the soil is simulated by an infinite element boundary. Traditionally, the boundary is cut off manually, and the waves are reflected on the boundary surface, returning energy to the analysis grid. The infinite element in ABAQUS can reduce the boundary effect by setting damping on the boundary [15-16]. Taking one-dimensional wave conduction as an example, suppose that the infinite element material in the dynamic analysis is linear.

$\rho, E, x, c,$tare density, elastic modulus, axial coordinate, wave speed, time.

$$c = \sqrt{\frac{E}{\rho}} \tag{4}$$

A damped boundary condition was set on the boundary,

$$\sigma = -d\frac{\partial u}{\partial t} = -d(-cf_1' + cf_2') \quad (5)$$

In order to achieve the phenomenon of no reflection, the following conditions must be met:

$$E(f_1' + f_2') + d(-cf_1' + cf_2') = 0 \quad (6)$$

Since no reflected waves appear, the following are obtained:

$$f_2 = 0, f_2' = 0 \quad (7)$$

The damping parameter can be solved from (6):

$$d = \rho c \quad (8)$$

This means that as long as the boundary damping parameters are chosen properly, the non-reflective situation can be simulated correctly.

The numerical model is shown in Figure 2.

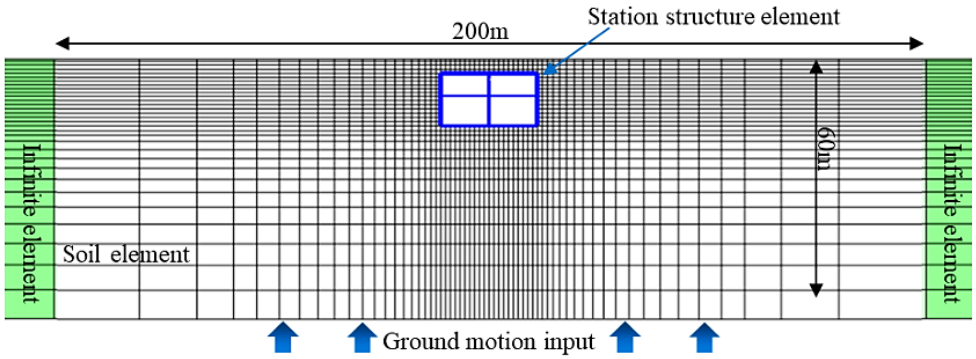

Figure 2. Finite-element model

The selected earthquake input at the bottom (i.e., the top of the bedrock) of the numerical model is the N-S component of El Centro ground motion, with its acceleration time history and Fourier amplitude spectrum shown in Figure 3. In order to investigate the acceleration response characteristics of the subway station structure under different seismic intensities, the peak ground accelerations at the bottom of the model are adjusted to 0.1, 0.2, 0.3, 0.4, 0.5, and 0.6 g separately.

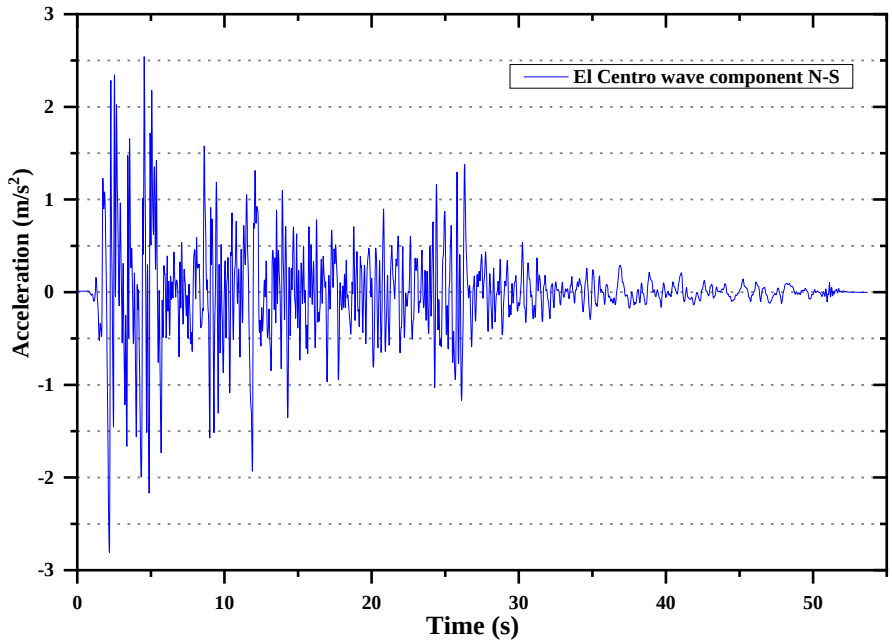

(a)

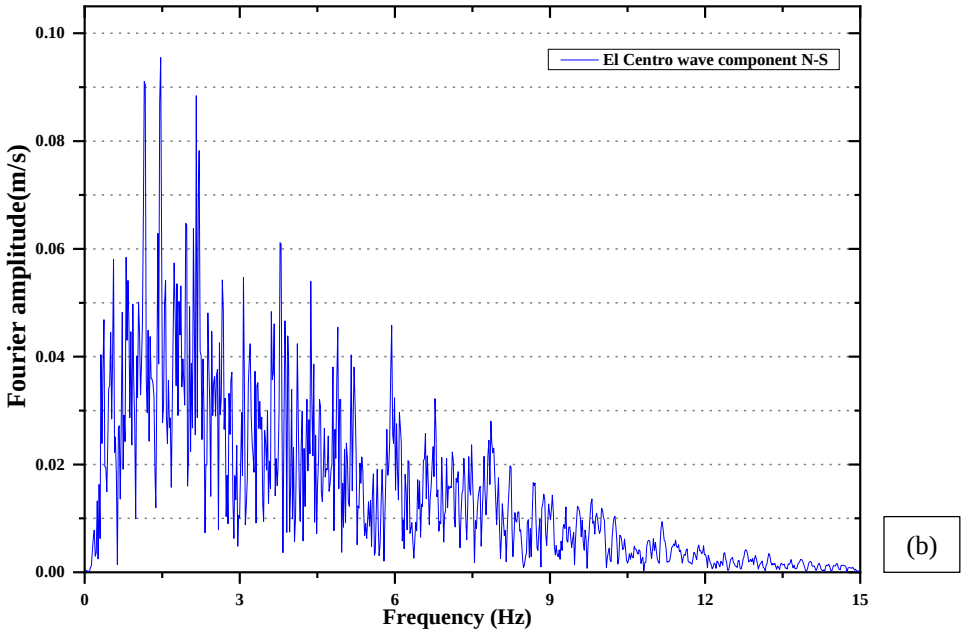

Figure 3. N-S component of El Centro ground motion: (a) Acceleration-time history (b) Fourier amplitude spectrum

4. Distribution of Peak Acceleration Responses in Structure

Figure 4 shows the distribution of peak acceleration responses at different locations of the subway station structure, as the peak input accelerations at the base are 0.1 and 0.6 g. It is seen in Figure 4(a) that when the ground motion intensity is low, the distribution of accelerations inside the subway station structure generally shows a gradually increasing trend from bottom to top, and the peak acceleration responses at the same height are practically the same. The locations corresponding to the maximum and minimum peak acceleration responses occur at the top and bottom plates, respectively. It is observed in Figure 4(b) that when the ground motion intensity is high the accelerations inside the subway station structure, in general, increase from bottom to top, with the location corresponding to the minimum peak acceleration response at the structural bottom plate, while the maximum peak acceleration response occurs at the upper-story central column.

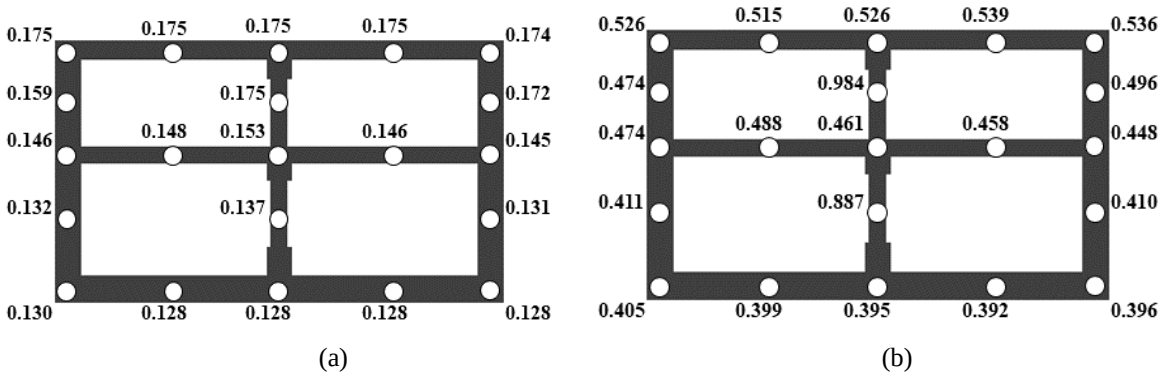

Figure 4. Peak acceleration responses at different locations of the structure: (a) 0.1g (b) 0.6g

Figure 5 shows the variations of peak acceleration responses of the bottom plate, middle plate, top plate, upper- and lower-story central columns, and ground surface as the peak of bedrock input acceleration changes. When the bedrock input accelerations are small (0.1 and 0.2 g), the accelerations inside the structure are close to the peak ground acceleration response due to the shallow-buried depth of the station. For the case of 0.1 g input, the amplification factors of peak accelerations at the bottom plate, lower central column, middle plate, upper central column, top plate, and ground surface relative to bedrock are 1.28, 1.37, 1.46, 1.75, 1.75, and 1.54, respectively. However, when the bedrock input acceleration is large (the cases of 0.3–0.6 g), the acceleration responses at the bottom, middle, and top plates are either less than or close to the peak ground acceleration response, and the peak acceleration responses of both upper and lower central columns significantly exceed the peak ground acceleration response. Specifically, for the case of 0.6 g, the amplification factors of peak accelerations at the bottom plate, lower central column, middle plate, upper central column, top plate, and ground surface relative to bedrock are 0.66, 1.48, 0.77, 1.64, 0.88, and 0.88, respectively. These results suggest that, because the dynamic response of the subway station structure is controlled by the deformation of the

surrounding soil, the overall distribution of peak interior acceleration responses of the subway station structure is similar to the pattern of acceleration propagation in soil, demonstrating the amplification effect under small earthquakes and the attenuation effects under large earthquakes. The reason why the acceleration response of the central column is significantly larger under large earthquakes is discussed in detail below.

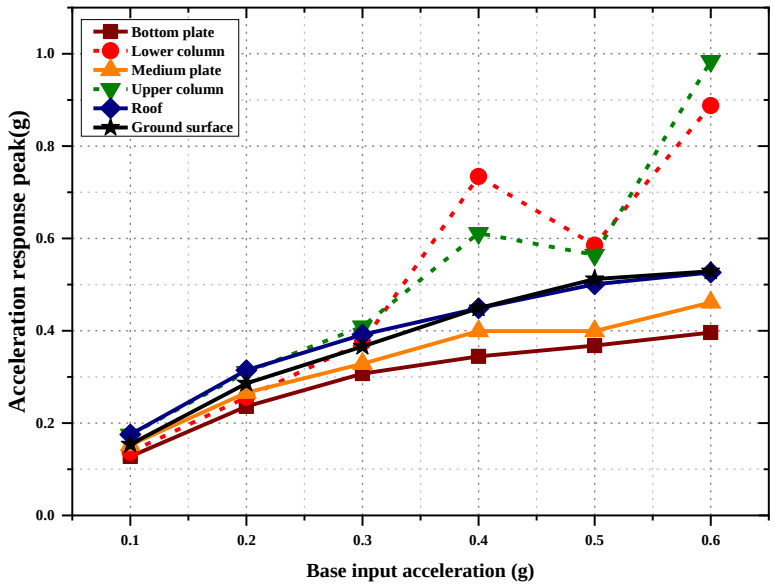

Figure 5. Peak acceleration responses with different base input accelerations

Figure 6 and 7 compare the acceleration-time histories and Fourier amplitude spectra, respectively, of the structural top plate and upper central column as well as the bedrock. It can be seen in Figure 6(a) that, when the peak input acceleration of the bedrock is 0.1 g, the accelerations of the top plate and the upper central column relative to that of bedrock are magnified, and the acceleration-time-history curves associated with these two locations are highly correlated, with corresponding peaks almost coinciding with each other. However, it is observed in Figure 6(b) that, when the peak input acceleration of the bedrock is 0.6 g, the acceleration-response-time history of the top plate is significantly smaller than that of bedrock, while the acceleration-response-time histories of the upper central column and the bedrock are very similar, with the peak acceleration of the central column more pronounced. Such phenomena are also observed by comparing the Fourier amplitude spectra in Figure 7. Figure 7(a) and 7(b) show that the acceleration Fourier amplitudes of the top plate and the upper central column are both magnified in the frequency range 0–3 Hz and attenuated in the frequency range 3–6 Hz. The differences between the two sets of acceleration Fourier amplitudes are as follows. For frequencies higher than 6 Hz, when the bedrock input acceleration is 0.1 g, the two sets of acceleration Fourier amplitudes are almost zero. In comparison, when the bedrock input acceleration is 0.6 g, the acceleration Fourier amplitudes of the top plate are also almost attenuated to zero while the acceleration Fourier amplitudes of the upper central column are still non-zero. Therefore, the higher-than-6-Hz frequency component is responsible for the high acceleration response of the central column compared to that of the top plate.

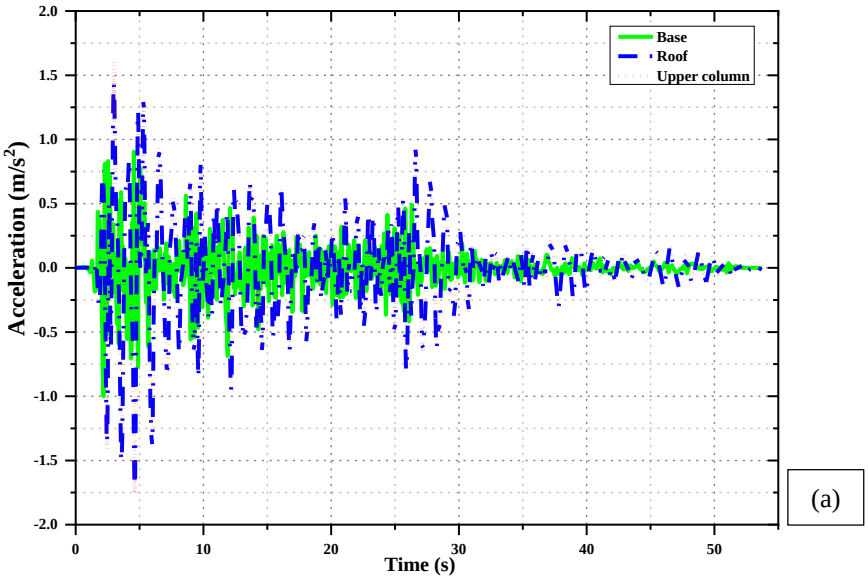

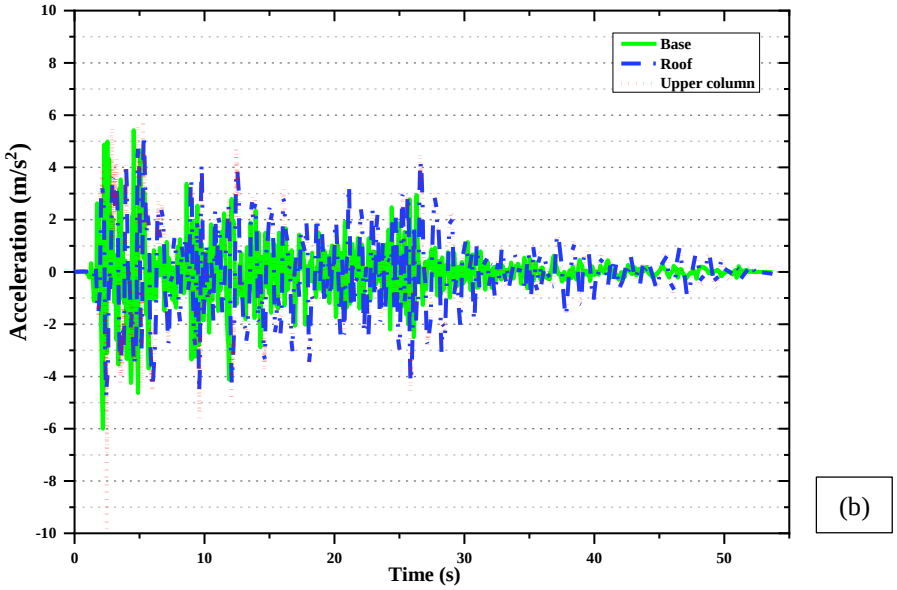

Figure 6. Comparison of acceleration-time histories for different locations: (a) 0.1 g, (b) 0.6 g

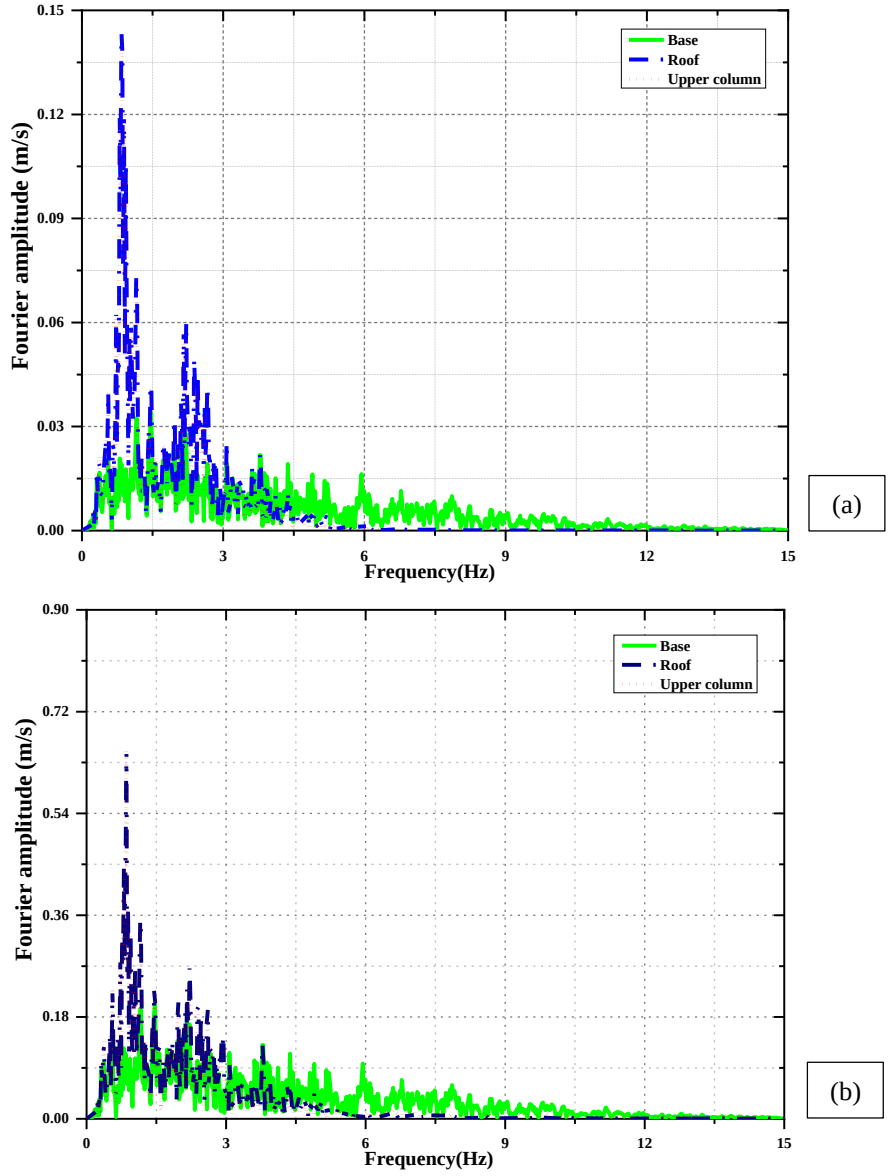

Figure 7. Comparison of acceleration Fourier amplitude spectra for different locations: (a) 0.1 g, (b) 0.6 g

The high-frequency acceleration response of the central column under strong ground motion is attributed to its weakened end restraints. As the weakest member of the subway station structure, the central column often suffers from the most severe plasticity developed at its ends under strong earthquakes, thereby affecting its acceleration response. Table 1 gives the plastic damage factors of the top and bottom ends of the upper central column as its peak acceleration occurs. When the bedrock input acceleration is 0.1 g, the damage factors of the top and bottom of the column are both close to zero, indicating that there is almost no plastic damage. In comparison, when the bedrock input acceleration is 0.2 g, the plastic damage at the top of the column is severe, while almost no plasticity occurs at the bottom of the column. Note that the acceleration responses of the central column under the above two bedrock-input-acceleration cases are not significantly large. When the bedrock input acceleration is in the range 0.3–0.6 g, severe plastic damage occurs at both the top and bottom of the central column. In particular, with the bedrock input acceleration in the range 0.4–0.6 g, the tensile damage factor exceeds 0.9. Under the four (0.3, 0.4, 0.5, and 0.6 g) input acceleration cases, the acceleration responses of the central column are obviously large. This observation indicates that the more severe the plastic damages at the two ends of the central column are, the weaker its two end constraints become, and hence the larger its acceleration response.

Table 1. Plastic damage factors for column ends corresponding to occurrence of peak acceleration of upper central column

Bedrock input acceleration (g)		0.1	0.2	0.3	0.4	0.5	0.6
Occurrence time of peak acceleration (s)		4.64	4.64	4.57	4.90	5.32	2.41
Column top	Tensile damage	0.04	0.77	0.96	0.99	0.99	0.97
	Compressive damage	0	0.2	0.44	0.84	0.94	0.49
Column bottom	Tensile damage	0	0.06	0.47	0.90	0.97	0.94
	Compressive damage	0	0	0.12	0.23	0.42	0.27

5. Nonstructural Damage Evaluation Based on Structural Acceleration Response

Because the nonstructural facilities are usually attached to horizontal structural members, such as floor plates, vertical structural members such as the central column are not considered when evaluating the damage to nonstructural members. Figure 8 shows the variation of peak acceleration responses of the structural bottom, middle, and top plates as the bedrock input acceleration changes. To investigate the effects of soil-layer stiffness on the acceleration of the subway station structure, two additional soil-layer shear-wave velocities (100 and 300 m/s) of the soil layer are considered in the calculation, and the results along with those calculated earlier with 200 m/s are plotted in Figure 8. It can be seen that, as the peak input acceleration of the bedrock increases, the peak acceleration responses of the structural bottom, middle, and top plates increase. In addition, as the soil-layer stiffness increases, the acceleration response of the structure also increases. This observation indicates that the higher the soil-layer stiffness of the site is, the larger the acceleration response of the subway station structure becomes, possibly causing more severe damage to nonstructural facilities.

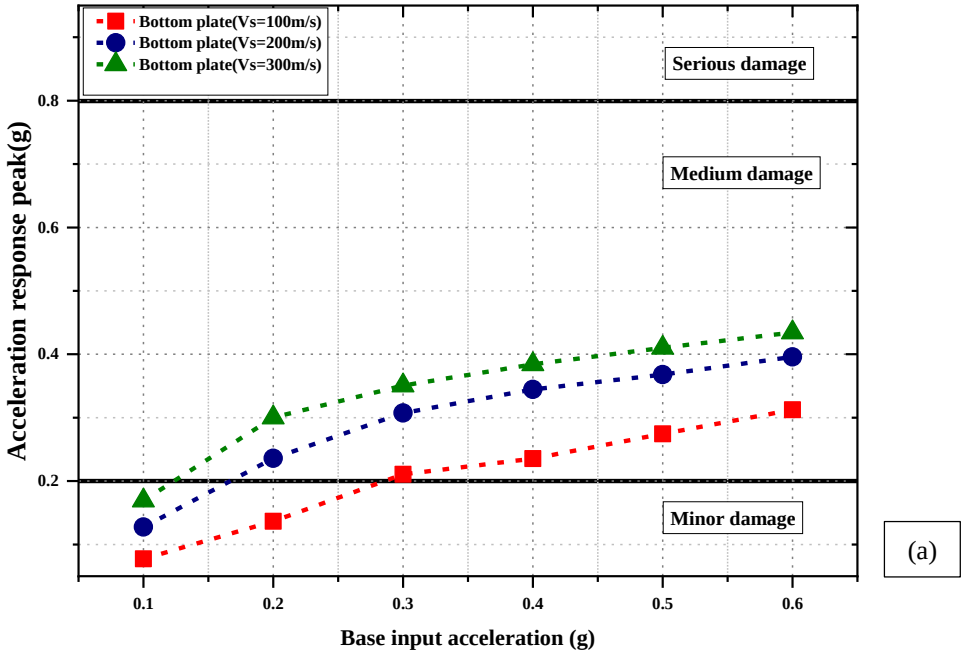

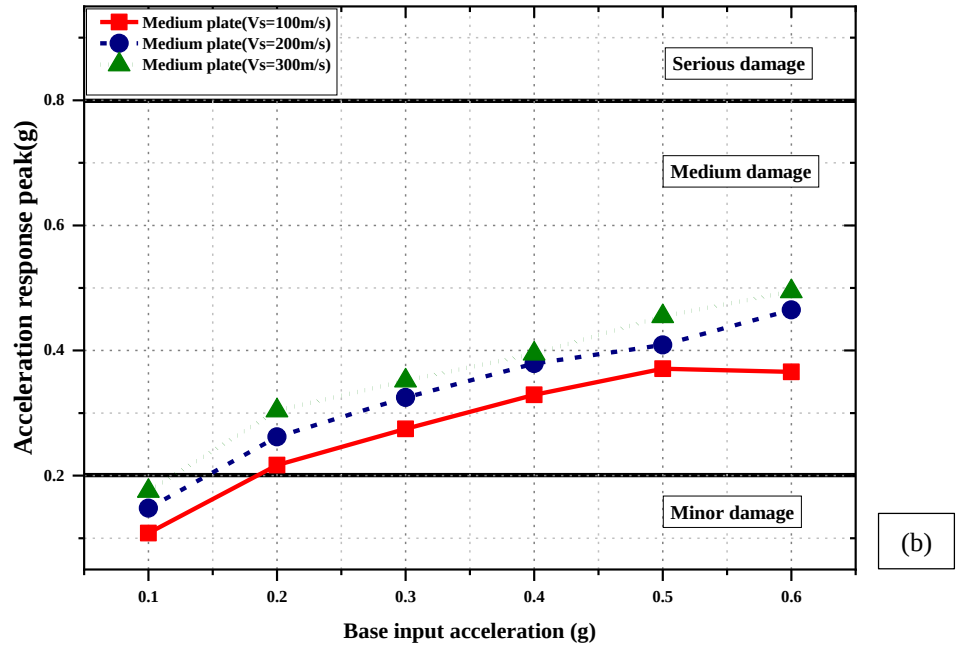

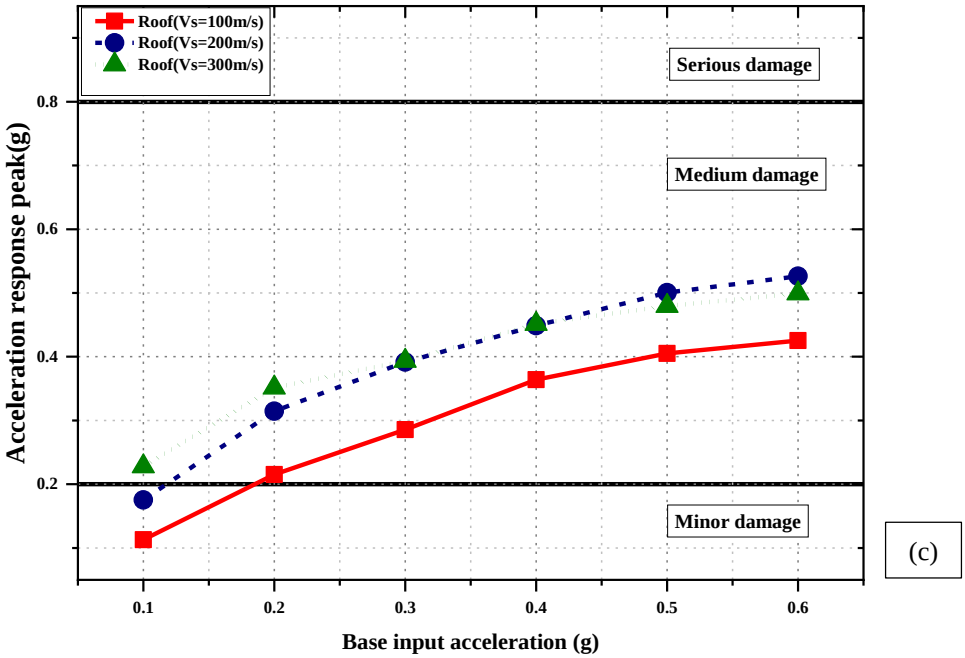

Figure 8. Peak acceleration responses at: (a) bottom (b) medium (c) roof

The relationship between structural acceleration response and nonstructural damage, according to that available in the literature [14], states that the nonstructural facilities are slightly damaged, moderately damaged, and severely damaged when the corresponding acceleration response is less than 0.2 g, in the range 0.2–0.8 g, and in the range 0.8–1.25 g, respectively. The nonstructural facilities are considered completely destroyed when their acceleration response is greater than 1.25 g. It can be seen in Figure 8 that the nonstructural facilities are slightly damaged and moderately damaged when the bedrock input accelerations are 0.1 g and in the range 0.2–0.6 g, respectively.

Under seismic ground motion, the acceleration response of an above-ground structure often exceeds ground acceleration and can be further amplified due to the whiplash effect. Therefore, it is unsuitable for the peak ground acceleration to be used as an index to evaluate the damage to above-ground nonstructural facilities. However, because the subway station structure is restrained by the soil layer, its acceleration response usually does not exceed the ground acceleration. Table 2 lists the percentage differences between the peak ground acceleration response and the peak acceleration responses at different locations of the station structure, with a positive percentage value denoting that the peak ground acceleration response is greater than the peak structural acceleration response. It is seen in Table 2 that there is a difference of −15% to 40% between the peak accelerations of the structure (at the top, middle, and bottom plates) and the ground. Therefore, the peak ground acceleration can be directly used as a fairly accurate, simple, and

practical index to evaluate the seismic damage to nonstructural facilities in a shallow-buried subway station structure.

Table 2. Percentage differences between peak ground acceleration and peak acceleration responses at different locations

Bedrock input acceleration (g)		0.1	0.2	0.3	0.4	0.5	0.6
Vs=100 m/s	Top plate	5%	7%	13%	7%	9%	16%
	Middle plate	14%	11%	18%	11%	21%	29%
	Bottom plate	35%	40%	37%	38%	37%	38%
Vs=200 m/s	Top plate	−13%	−9%	−6%	1%	3%	0
	Middle plate	4%	8%	11%	16%	20%	12%
	Bottom plate	17%	17%	16%	23%	12%	25%
Vs=300 m/s	Top plate	−14%	−6%	11%	−2%	1%	6%
	Middle plate	12%	8%	20%	11%	11%	14%
	Bottom plate	15%	9%	21%	13%	15%	18%

6. Conclusions

Using the finite-element software ABAQUS, a dynamic soil-structure interaction model has been established for a two-story subway station structure. The distribution of peak acceleration responses of the structure has been analysed, and the non-structural damage evaluation has been carried out based on the structural acceleration response. Major conclusions are drawn as follows.

- The peak acceleration responses inside the subway station structure generally increase from the bottom to top of the structure, and the peak acceleration responses at the same height are practically equal.
- Under weak ground motion, the maximum peak acceleration response inside the subway station structure occurs at the top plate. Under strong ground motion, such a maximum peak response takes place in the central column and is attributed to its weakened end restraints due to the occurrence of severe plastic damage there.
- In general, non-structural facilities are slightly damaged when the bedrock input acceleration is 0.1 g, and are moderately damaged when the bedrock input acceleration is in the range 0.2–0.6 g.
- Higher stiffness of site soil layer leads to larger acceleration response of the subway station structure and hence likely more severe damage to non-structural members.
- The peak accelerations inside a shallow-buried subway station structure are generally less than or close to the peak ground acceleration. The difference between the peak accelerations of the structural top plate, middle plate, bottom plate, and the ground is approximately in the range 15–40%. Therefore, the peak ground acceleration can be directly used and is a fairly accurate, simple, and practical index for evaluating the seismic damage to nonstructural facilities of shallow-buried subway station structures.

7. Conflicts of Interest

The authors declare no conflict of interest.

8. References

[1] An X., Shawky A. A., Maekawa, K. “The collapse mechanism of a subway station during the Great Hanshin earthquake”. Cement and concrete composites, No.3 (1997): 241-257. doi: 10.1016/s0958-9465(97)00014-0.

[2] Yang, C. “Earthquake damage analysis of the subway project of the Hanshin earthquake in Japan”. Earthquake Resistant Engineering, No.2 (1996): 40-42. doi: 10.16226/j.issn.1002-8412.1996.02.011.

[3] X. l. Du, Y. Li, C. S. Xu, etc. "Review on damage causes and disaster mechanism of Daikai subway station during 1995 Osaka-Kobe Earthquake." Chinese Journal of Geotechnical Engineering, 2018(2): p. 223-236. doi: 10.11779/CJGE201802002.

[4] Chen, Zhiyi, Wei Chen, Yueyang Li, and Yong Yuan. “Shaking Table Test of a Multi-Story Subway Station under Pulse-Like Ground Motions.” Soil Dynamics and Earthquake Engineering 82 (March 2016): 111–122. doi:10.1016/j.soildyn.2015.12.002.

[5] D. Z. Quan, Y. H. Wang, D. Ye, etc. “Shaking table test study on subway station built in loess area”. China Civil Engineering Journal, 2016(11): p.79-90. doi: 10.15951/j.tmgcxb.2016.11.009

[6] J. J. Lv， Z. Q. Zhao. “Seismic Analysis of Typical Subway Station Structure of Tianjin Metro Line 10. Journal of Railway Engineering Society, 2015 (10): p.126-130.

[7] P. F. Li, Q. J. Chen. “Response of Subway Station and Site to Multi-Dimensional Seismic Waves”. Chinese Quarterly of Mechanics, 2015(04): p.636-644. doi: 10.15959/j.cnki.0254-0053.2015.04.010.

[8] H. Z. Zhou, G. Zheng, X. Q. Li, etc. “Nonlinear Seismic Responses Analysis of Subway Structure in Soft Soil”. Journal of Tianjin University (Science and Technology), 2016(04): p.361-368. doi: 10.11784/tdxbz201407070.

[9] H. Y. Zhuang, X. J. Wang, R. Wang, etc. “Characteristics of lateral deformation of soil-subway dynamic interaction system”. Chinese Journal of Geotechnical Engineering, 2017(10): p.1761-1769. doi: 10.11779/CJGE201710002.

[10] D. Z. Quan, Y. H. WANG, Y. L. Jing, etc. “Infinite element transmitting Boundary in dynamic analysis of subway station in loess area”. J. Xi'an Univ. Of Arch. & Tech. (Natural Science Edition), 2015(04): p537-542. doi: 10.15986/j.1006-7930.2015.04.013.

[11] Y.L. Zheng, L.D. Yang, Earthquake damage of underground structures and earthquake countermeasures. Earthquake Resistant Engineering, 1999(4): p. 21-26. doi:10.16226/j.issn.1002-8412.1999.04.005.

[12] Li, B., J.B. Liu and X.Q. Liu, Strong Earthquake Response Analysis and Design of Ground Motion Parameters for Metro Stations. Earthquake Engineering and Engineering Dynamics, 2008(1): p. 17-23. doi:10.13197/j.eeev.2008.01.006.

[13] Elenas, A. and K. Meskouris, Correlation study between seismic acceleration parameters and damage indices of structures. Engineering Structures, 2001(6): p. 698-704. doi: 10.1016/S0141-0296(00)00074-2.

[14] Gunturi, S. and H. Shah. Building specific damage estimation. in Earthquake Engineering: Proceedings of the Tenth World Conference on Earthquake Engineering. 1992.

[15] Ministry of Housing and Urban-Rural Development of the People's Republic of China, Code for seismic design of buildings, in GB50011-2010. 2010, China Building Industry Press: Beijing.

[16] Xia, C., Zhao, B.M., Wang, Z., Sun, F.B.“Factors affecting cross-section deformation of subway stations under earthquake”. Chinese Civil Engineering Journal, No. S1 (2015): 132-136.

[17] Li, W. T., Chen, Q. J. “Seismic performance and failure mechanism of a subway station based on nonlinear finite element analysis”. KSCE Journal of Civil Engineering, No. 2(2018): 765–776. doi 10.1007/s12205-017-1840-y.

[18] Dong, Z. F., Wang, J. J., Yao, Y. C. “Research on the seismic performance index system of urban mass transit underground structures"Earthquake Engineering and Engineering Vibration, No.S1(2014): 699-705. doi: 10.13197/j.eeev.2014.S0.699.dongzf.109.

[19] Wang, G. B., Xie, W. P., Sun, M., Liu, W. G. “Evaluation method for seismic behaviors of underground frame structures”. Chinese Journal of Geotechnical Engineering, N0.4 (2011): 593-598.

[20] Ministry of Housing and Urban-Rural Development of the People's Republic of China. Code for design of condret structures (GB50010-2010): 207-220.